Directional control of spin-wave emission by spatially shaped light

Takuya Satoh[1,2#*], Yuki Terui[1#], Rai Moriya[1], Boris A. Ivanov[1,3], Kazuya Ando[4], Eiji Saitoh[4,5,6,7], Tsutomu Shimura[1] and Kazuo Kuroda[1]

[1] *Institute of Industrial Science, The University of Tokyo, Tokyo 153-8505, Japan*

[2] *PRESTO, Japan Science and Technology Agency, Tokyo 102-0076, Japan*

[3] *Institute of Magnetism, NASU, 03142 Kiev, Ukraine*

[4] *Institute for Materials Research, Tohoku University, Sendai 980-8577, Japan*

[5] *CREST, Japan Science and Technology Agency, Tokyo 102-0075, Japan*

[6] *The Advanced Science Research Center, Japan Atomic Agency, Tokai 319-1195, Japan*

[7] *WPI-Advanced Institute for Materials Research, Tohoku University, Sendai 980-8577, Japan*

[#]*These authors contributed equally to this work*

[*]*e-mail: tsatoh@iis.u-tokyo.ac.jp*

In future spintronics it is anticipated that spin waves will function as unique information carriers that are free from Joule heating[1–7]. Directional control of spin-wave emission has been desired for the realization of switching devices. Here, we propose a promising technique that makes use of a spatially shaped light pulse with circular polarization. Focusing this light pulse on a magnet generates spin waves via the inverse Faraday effect. Moreover, the wavenumber distribution of the spin waves is determined by the spatial intensity distribution of the light spot. We demonstrate the principle of this technique both theoretically and experimentally. We successfully control the direction of the energy flow by shaping the light spot into an ellipse, with its major axis parallel or perpendicular to the magnetic field. Our findings will open up the possibility of fast and arbitrary synthesis of spin-wave patterns by using a more sophisticated light-shaping technique, for example using a computer-generated hologram[8].

To date, spin waves have been excited by a harmonic or pulsed microwave field emitted from a microstrip antenna[9-17] and by the transfer of spin angular momentum from conduction electrons to localized electrons—the so-called spin transfer torque[7,18-20]. However, once the antenna and the electrode have been fabricated and the magnetic field has been oriented, the propagation characteristics of the spin waves are not directly tunable.

The thermal emission of spin waves by ultrashort light pulses has been observed indirectly[6,21] and, recently, a non-thermal method of magnetization control by ultrashort light pulses has also been reported[22]. This latter method makes use of the inverse Faraday effect, whereby a circularly polarized light pulse generates an effective magnetic field along the beam direction. The inverse Faraday effect has been described as impulsive stimulated Raman scattering[23], suggesting the possibility of ultrafast magnetic switching. So far, discussion has been limited to local spin precessions only. Non-local spin precessions—that is, propagating spin waves—excited by this non-thermal and impulsive excitation method have never been observed. However, in contrast to other excitation method, this method enables the realization of two-dimensional emission of spin waves from a focused light spot in a non-contact manner, as well as the possibility of broadband spin excitation in the wavenumber and energy spectra.

We measured the magneto-optical Faraday rotation of a probe pulse to monitor time- and space-resolved spin waves in a ferrimagnetic insulator, $Gd_{4/3}Yb_{2/3}BiFe_5O_{12}$, excited by a femtosecond pump pulse. A schematic of the sample geometry and pump–probe beams is shown in Fig. 1a (see Methods).

Figure 1b presents polarization rotation of the probe pulse versus the time delay between the pump and probe pulses when the spots of these pulses overlap spatially. The amplitude of the spin precession is estimated to be ~1°. The initial phase of the spin precession shifts by π radians when the helicity of the pump pulse is reversed. This is clear evidence of the inverse Faraday effect, where the direction of the magnetic field is determined by the pump helicity[22]. Because the direction of the effective magnetic field pulse $\mathbf{h}(x, y, t) = \mathbf{h}(\mathbf{r}, t)$ generated via the inverse Faraday effect is perpendicular to the sample surface, the oscillations show sinusoidal dependence. The thermal effect caused by the light illumination is discussed in Supplementary Section S1a. Figure 1c shows the Fourier-transform amplitude spectrum (green circles) of this oscillation after subtracting the incoherent offset. For comparison, the absolute value of the complex permeability obtained in a ferrimagnetic resonance experiment, indicating uniform spin precession ($\mathbf{k} = 0$), is also plotted (black circles). The full-width at half-maximum (FWHM) of the pump pulse-induced spin precession is broader than that of the uniform spin precession. This difference suggests that the energy and angular momentum have been emitted away from the pump spot ($r_0 = 25$ μm) in the form of spin waves. Furthermore, the centre frequency of the oscillation ($f_{pp} = 2.6$ GHz) is lower than the uniform precession frequency ($f_{FMR} = 3.6$ GHz); that is, $f_{pp} < f_{FMR}$. This implies that the excited spin wave is a backward volume magnetostatic wave (BVMSW)[2,3], which is characterized by its dispersion curve having a negative slope as a result of a magnetic dipolar interaction. This characteristic can be observed in Fig. 1d, which plots constant-frequency contours in the k_x–k_y plane of the lowest-order BVMSW[24].

In contrast to direct spin excitation by a microwave field[9-17], the mechanism of spin excitation by a femtosecond light pulse is still not fully understood[6,21-23]. Here, we offer a simple model in which the source of the spin wave in **k**-space, $h(\mathbf{k})$, is determined by the Fourier transform of the spatial intensity distribution of the pump spot, $|E(r)|^2 \approx \exp(-r^2/2r_0^2)$. The out-of-plane component of the induced magnetization, m_z, is then given by a two-dimensional integration over all excited $\mathbf{k} = (k_x, k_y)$ (Supplementary Section S1b):

$$m_z(\mathbf{r},t) \propto \int d\mathbf{k} h(\mathbf{k}) \sin\left(\mathbf{k}\cdot\mathbf{r} - \omega(\mathbf{k})t\right) \exp\left(-\alpha\omega(\mathbf{k})t\right). \quad (1)$$

Here, the cutoff wavenumber k_c is determined so as to satisfy $\exp(-k_c^2 r_0^2/2) \ll 1$, and $\omega(\mathbf{k}) = 2\pi f(\mathbf{k})$ is the lowest order of the BVMSW dispersion, as shown in Fig. 1d. Gilbert damping is included in $\exp(-\alpha\omega(\mathbf{k})t)$, where parameter $\alpha = 0.02$ is determined by a ferrimagnetic resonance experiment (see Methods). The numerical results of $m_z(\mathbf{r} = 0, t)$ obtained using $\alpha = 0.02$ and $r_0 = 25$ μm are shown in Fig. 1b. The calculation shows excellent agreement with the experiment. Fourier-transform amplitude spectra with $\alpha = 0$, 0.02 and 0.05 and $r_0 = 25$ μm are plotted in Fig. 1c. The curve with $\alpha = 0.02$ (±0.01) shows the best agreement with the pump–probe experiment, but these three curves are somewhat similar. This similarity suggests that the contribution to the FWHM of the pump pulse-induced spin precession is dominated by the emission of the spin wave out of the pump spot, or in other words, dephasing, rather than the intrinsic Gilbert damping, represented by α. Note that when the pump spot size is sufficiently large ($r_0 = 2.5$ mm), which means that spin waves with approximately $\mathbf{k} = 0$ are excited, the Fourier-transform amplitude spectrum of the calculated waveform coincides with the absolute value of the permeability (Fig. 1c). Therefore, we have confirmed that our model can reproduce both

pump pulse-induced spin precession and uniform spin precession by choosing r_0 appropriately.

To confirm the spin-wave emission, we performed pump–probe measurements by scanning the pump spot in the *x*-direction. In the following, the pump helicity is assumed to be fixed at $\sigma(+)$. Figure 1e shows a spatiotemporal map of the spin waves. The incoherent offset appearing at the pump spot has been subtracted. Spin waves have been emitted from the pump spot. In contrast, the wave front has moved toward the pump position from the outside (Supplementary Movie S1). Once again, this confirms the backward nature of the BVMSW. The propagation of spin waves with a wavelength of 200–300 μm was observed. The experimental results in Fig. 1e are in excellent agreement with the results calculated using equation (1) (shown in Fig. 1f), indicating that the probe spot size is small enough to resolve the waveform.

To obtain a two-dimensional map of the spin-wave emission we conducted pump–probe measurements by scanning the pump spot two-dimensionally, then performed calculations under the same conditions (Fig. 2a,b) with the time delay fixed at 1.5 ns. In Fig. 2a (and also in Figs. 3b,e), the incoherent offset at the pump spot was not subtracted. The wavefront was not circular, reflecting the anisotropic property of the spin-wave dispersion. The emission was symmetric (in amplitude and phase) with respect to the *x*-and *y*-axes, unlike excitation by a microwave field emitted from a microstrip antenna[14]. This is because the direction of the effective magnetic field due to the inverse Faraday effect is perpendicular to the sample surface, which affects the magnetization symmetrically about the pump spot. Again, the experimental and calculated results are in satisfactory agreement.

The amplitude map in Fig. 2c is extracted from Fig. 2b. The spin waves are focused at angles 0° and approximately ±30° with respect to the *x*-axis. This focusing effect originates from the non-collinearity of the group and phase velocities as a result of the anisotropy of the spin wave dispersion relation. The phase velocity angle ϕ and group velocity angle θ, both with respect to the *x*-axis for a given frequency, are defined as $\phi = \tan^{-1}\left(k_y / k_x\right)$ and $\theta = \tan^{-1}\left(\frac{\partial f}{\partial k_y} \Big/ \frac{\partial f}{\partial k_x} \right)$, respectively. Relations between ϕ and θ are plotted in Fig. 2d for f = 2.2, 2.6 and 3.0 GHz. For f = 2.6 and 3.0 GHz, the direction of the group velocity is constant under the condition $d\theta/d\phi = 0$, which corresponds to the inflection points of the constant-frequency contour in the k_x–k_y plane (Fig. 1d). By integrating over ϕ, one can find the emission amplitude as a function of θ, as shown in Fig. 2e. Sharp peaks are obtained at $\theta \approx$ 180 ± 32°, 180 ± 22° and 180 ± 24° for f = 2.2, 2.6 and 3.0 GHz, respectively. For f = 2.6 GHz, there is also a broad peak at $\theta \approx$ 180°. Because the observed spin wave contains a broadband frequency component ranging over 5 GHz, in Fig. 2f we plot a contour plot of the emission amplitude. Peaks are located at about $\theta \approx$ 180 ± 30° over a broad spectral range. This clearly indicates that the spin-wave emission—that is, the energy flow—is self-focused (Supplementary Movie S2). The transverse size of the focused spin waves is comparable to the pump spot diameter (~50 μm) and does not suffer from diffraction. This phenomenon is analogous to the focusing of other waves, such as elastic waves[25] and electromagnetic waves[26] propagating in anisotropic crystals. We note that the focused spin waves are emitted in the form of bullets. This is attributed to spin-wave echo[5], which differs from the results of other studies using a microwave field or spin transfer torque[9,16,17,20,27]. We also note that a spin-

wave bullet is emitted at $\theta \approx 180°$. This may be due to the difference in group velocity between the spin waves propagating at $\theta \approx 180°$ and $180 \pm 30°$.

Now that the validity of the model in equation (1) has been confirmed numerically and experimentally, directional control of spin-wave emission by spatially shaped light pulses should be possible. The amplitude distribution of an electric field on the sample surface, $E(\mathbf{r})$, is given by the Fourier transform of the amplitude distribution of the electric field in the front focal plane of the lens, $E(\mathbf{r}')$[28]. Therefore, $h(\mathbf{k})$ should be determined by $E(\mathbf{r}')$. To demonstrate this idea experimentally, a rectangular aperture was placed in the front focal plane of the lens, as illustrated in Fig. 3a. The time delay was fixed at 1.5 ns. Two-dimensional maps of spin-wave emission are shown in Figs. 3b,e for cases where the longer side of the rectangle was parallel and perpendicular to the magnetic field, respectively. The corresponding maps obtained by calculation are shown in Fig. 3c,f. In the calculation, interference fringes due to Fraunhofer diffraction were neglected, and the spot shape on the sample surface was approximated as an ellipse. Comparisons of Fig. 3b and c and of Fig. 3e and f indicate that the model predicted the experiment with very good accuracy. We have clearly demonstrated that the properties of the excited spin waves can be controlled by using a rectangular aperture. When the longer side of the aperture is parallel to the magnetic field, the **k**-space distribution of the pump spot, which determines the **k**-space distribution of the induced spin wave, is an ellipse with the major axis parallel to the magnetic field. Accordingly, $|k_y|$ is restricted to a smaller value than $|k_x|$, as shown in Fig. 3b,c. The amplitude maps of Fig. 3c,f are plotted in Fig. 3d,g, respectively. In spite of the anisotropy of the spin-wave dispersion caused by the magnetic field, the direction of the spin-wave emission can be tuned by

rotating the direction of the rectangular aperture; specifically, the direction of energy flow is parallel to the longer side of the aperture (Supplementary Movie S3).

It is valid to view the elongated source as a coherent superposition of discrete point sources, which is analogous to the Huygens' principle of diffraction. Similar to the diffraction of light at a slit, the directivity of the spin-wave emission is improved as the length of the major axis increases. The interference pattern of Fresnel diffraction is smeared out because of the broadband spectrum of the emitted spin waves. This principle is so general that it can be applied to the control of other waves, such as elastic and electromagnetic waves.

METHODS

Sample.

Yttrium iron garnet (YIG) has often been used as a sample in spintronics because of its intrinsically low magnetic damping[5,7,9,12,14,17,27]. However for an experiment involving photo-induced spin waves, bismuth-doped rare-earth iron garnet is expected to be more suitable than YIG due to its high magneto-optical susceptibility[29]. We therefore used a single crystal of a ferrimagnetic insulator ($Gd_{4/3}Yb_{2/3}BiFe_5O_{12}$) with perpendicular anisotropy. The sample thickness was 110 μm. All measurements were performed at room temperature, which was below the Curie temperature of the sample (T_c = 573 K).

Sample characterization.

The ferrimagnetic resonance frequency (f_{FMR} = 3.6 GHz) was measured under an external in-plane magnetic field of H_0 = 1 kOe. The perpendicular anisotropy field was calculated to be H_u = 450 Oe from $f_{FMR} = \gamma\sqrt{H_0\{H_0 - H_u + 4\pi M_s(N_z - N_x)\}}$ [30], and the saturation magnetization $4\pi M_s$ = 1,140 G was determined using a superconducting quantum interference device. N_x and N_z are the demagnetizing factors along the x- and z-axes, respectively, and γ = 2.8 MHz Oe^{-1} is the electron gyromagnetic ratio. From the FWHM of the resonance peak (Δf_{FMR} = 75 MHz) we also determined the Gilbert damping coefficient to be $\alpha = \Delta f_{FMR} / f_{FMR} = 0.02$.

Pump–probe experimental set-up.

Linearly polarized pulses from a Ti:sapphire laser with a wavelength of 792 nm and a pulse width of 120 fs were used as the probe. Circularly polarized pulses with a wavelength of 1,400 nm, generated by an optical parametric amplifier, were used as the pump. Except for the experiments with the spatially shaped pump pulse, the pump and probe beams were focused on the sample to spot diameters of 50 and 40 μm, respectively. The spatially shaped pump pulse was provided using a rectangular aperture (6 mm × 1.2 mm) in the front focal plane of a focusing lens. The pump spot on the sample was elliptical, with a major radius of 140 μm and a minor radius of 35 μm. The pump fluence was 200 mJ cm^{-2}. An in-plane magnetic field of 1 kOe was applied to saturate the magnetization in the *x*-direction. The pump spot was scanned at intervals of 20 μm, and the position of the probe spot was fixed. Polarization rotation of the transmitted probe light was recorded for each pump position.

References

1 Maekawa, S. (ed.) *Concepts in Spin Electronics* (Oxford Univ. Press, 2006).

2 Gurevich, A. G. & Melkov, G. A. *Magnetization Oscillations and Waves* (CRC Press, 1996).

3 Stancil, D. D. & Prabhakar, A. *Spin Waves: Theory and Applications* (Springer, 2009).

4 Kruglyak, V. V., Demokritov, S. O. & Grundler, D. Magnonics. *J. Phys. D* **43**, 264001 (2010).

5 Serga, A. A., Chumak, A. V. & Hillebrands, B. YIG magnonics. *J. Phys. D* **43**, 264002 (2010).

6 Lenk, B., Ulrichs, H., Garbs, F. & Münzenberg, M. The building blocks of magnonics. *Phys. Rep.* **507**, 107–136 (2011).

7 Kajiwara, Y. *et al.* Transmission of electrical signals by spin-wave interconversion in a magnetic insulator. *Nature* **464**, 262–266 (2010).

8 Lee, W.-H. in *Progress in Optics* (ed. Wolf, E.) 121–232 (North-Holland, 1978).

9 Büttner, O. *et al.* Linear and nonlinear diffraction of dipolar spin waves in yttrium iron garnet films observed by space- and time-resolved Brillouin light scattering. *Phys. Rev. B* **61**, 11576–11587 (2000).

10 Park, J. P., Eames, P., Engebretson, D. M., Berezovsky, J. & Crowell, P. A. Spatially resolved dynamics of localized spin-wave modes in ferromagnetic wires. *Phys. Rev. Lett.* **89**, 277201 (2002).

11 Covington, M., Crawford, T. M. & Parker, G. J. Time-resolved measurement of propagating spin waves in ferromagnetic thin films. *Phys. Rev. Lett.* **89**, 237202 (2002).

12 Wu., M. Z., Kalinikos, B. A., Krivosik, P. & Patton, C. E. Fast pulse-excited spin waves in yttrium iron garnet thin films. *J. Appl. Phys.* **99**, 013901 (2006).

13 Liu, Z., Giesen, F., Zhu, X., Sydora, R. D. & Freeman, M. R. Spin wave dynamics and the determination of intrinsic damping in locally excited permalloy thin films. *Phys. Rev. Lett.* **98**, 087201 (2007).

14 Schneider, T., Serga, A. A., Neumann, T., Hillebrands, B. & Kostylev, M. P. Phase reciprocity of spin-wave excitation by a microstrip antenna. *Phys. Rev. B* **77**, 214411 (2008).

15 Perzlmaier, K., Woltersdorf, G. & Back, C. H. Observation of the propagation and interference of spin waves in ferromagnetic thin films. *Phys. Rev. B* **77**, 054425 (2008).

16 Demidov, V. E. *et al.* Radiation of spin waves from the open end of a microscopic magnetic-film waveguide. *Phys. Rev. B* **80**, 014429 (2009).

17 Schneider, T. *et al.* Nondiffractive subwavelength wave beams in a medium with externally controlled anisotropy. *Phys. Rev. Lett.* **104**, 197203 (2010).

18 Kiselev, S. I. *et al.* Microwave oscillations of a nanomagnet driven by a spinpolarized current. *Nature* **425**, 380–383 (2003).

19 Boulle, O. *et al.* Shaped angular dependence of the spin-transfer torque and microwave generation without magnetic field. *Nature Phys.* **3**, 492–497 (2007).

[20] Demidov, V. E., Urazhdin, S. & Demokritov, S. O. Direct observation and mapping of spin waves emitted by spin-torque nano-oscillators. *Nature Mater.* **9**, 984–988 (2010).
[21] van Kampen, M. *et al.* All-optical probe of coherent spin waves. *Phys. Rev. Lett.* **88**, 227201 (2002).
[22] Kimel, A. V. *et al.* Ultrafast non-thermal control of magnetization by instantaneous photomagnetic pulses. *Nature* **435**, 655–657 (2005).
[23] Kirilyuk, A., Kimel, A. V. & Rasing, Th. Ultrafast optical manipulation of magnetic order. *Rev. Mod. Phys.* **82**, 2731–2784 (2010) and references therein.
[24] Hurben, M. J. & Patton, C. E. Theory of magnetostatic waves for in-plane magnetized anisotropic films. *J. Magn. Magn. Mater.* **163**, 39–69 (1996).
[25] Taylor, B., Maris, H. J. & Elbaum, C. Phonon focusing in solids. *Phys. Rev. Lett.* **23**, 416–419 (1969).
[26] Chigrin, D. N. Radiation pattern of a classical dipole in a photonic crystal: Photon focusing. *Phys. Rev. E* **70**, 056611 (2004).
[27] Veerakumar, V. & Camley, R. E. Magnon focusing in thin ferromagnetic films. *Phys. Rev. B* **74**, 214401 (2006).
[28] Hecht, E. *Optics* 4th edn (Addison-Wesley, 2002).
[29] Zvezdin, A. K. & Kotov, V. A. *Modern Magnetooptics and Magnetooptical Materials* (Institute of Physics, 1997).
[30] Farle, M. Ferromagnetic resonance of ultrathin metallic layers. *Rep. Prog. Phys.* **61**, 755–826 (1998).

Acknowledgements

The authors thank S. O. Demokritov, K. Sawada and A. Koreeda for valuable discussions, R. Iida and I. Yoshimine for technical assistance, and S. Takeda for the ferrimagnetic resonance measurements. This work was supported by KAKENHI 23104706 and Japan Science and Technology Agency (JST)—Precursory Research for Embryonic Science and Technology (PRESTO) (T. Satoh), National Academy of Sciences of Ukraine (NASU) 220-10 and Scientific and Technological Center of Ukraine (STCU) 5210 (B.A.I.). B.A.I. was supported by the Japan Society for the Promotion of Science (JSPS), Invitation Fellowship Programs for Research in Japan.

Author contributions

T.Satoh and R.M. initiated this study. T.Satoh and Y.T. planned this study, carried out the experiment, calculation and analysis, and wrote the manuscript. B.A.I. provided the theoretical model and wrote Supplementary Section S1b. K.A. and E.S. contributed to sample characterization. T.Shimura and K.K. supervised this study. All authors discussed the results and commented on the manuscript.

Additional information

Supplementary information is available in the online version of the paper. Reprints and

permission information is available online at http://www.nature.com/reprints. Correspondence and requests for materials should be addressed to T. Satoh.

Competing financial interests

The authors declare no competing financial interests.

Figure Captions

Figure 1

Pump pulse-induced spin waves in comparison with ferrimagnetic resonance.

a, Experimental configuration. **b**, Time-resolved magneto-optical Faraday rotation waveforms when pump spot and probe spot overlap spatially. Red and blue circles represent pump helicities σ (+) and (−), respectively. Solid curves represent numerical results with α = 0.02. **c**, Green circles: Fourier-transform amplitude spectrum of the oscillation in **b**. Black circles: absolute value of complex permeability obtained by a ferrimagnetic resonance experiment. Red, green and purple curves: numerical results with α = 0, 0.02 and 0.05, respectively, and r_0 = 25 μm. Blue curve: numerical result with α = 0.02 and r_0 = 2.5 mm. **d**, Constant-frequency contours in k_x–k_y plane for various frequencies. Blue and red arrows: directions of phase and group velocities, respectively. **e**,**f**, Spatiotemporal maps of spin waves when scanning parallel to the *x*-axis, obtained by experiment (**e**) and calculation (**f**).

Figure 2

Two-dimensional maps of spin-wave emission.

a,**b**, Two-dimensional maps of spin-wave emission obtained by experiment (**a**) and calculation (**b**). **c**, Amplitude map extracted from **b**. Dotted lines are directed at 0° and ±30° with respect to the *x*-direction. **d**, Relationship between ϕ and θ for f = 2.2, 2.6 and

3.0 GHz, derived from the spin-wave dispersion calculated using the method reported in ref. 24. **e**, Emission amplitude as a function of θ. **f**, Contour plot of the emission amplitude for f and θ.

Figure 3

Two-dimensional maps of spin wave emitted by a spatially shaped light pulse.

a, Pumping geometry with a rectangular aperture (6 mm × 1.2 mm). Lens focal length = 25 cm. **b**,**c**, Two-dimensional maps of spin-wave emission obtained by experiment (**b**) and calculation (**c**). The longer side of the aperture is parallel to the *x*-axis. **d**, Amplitude map of spin-wave emission extracted from **c**. **e**,**f**, Two-dimensional maps of spin-wave emission obtained by experiment (**e**) and calculation (**f**). The longer side of the aperture is parallel to the *y*-axis. **g**, Amplitude map of spin-wave emission extracted from **f**.

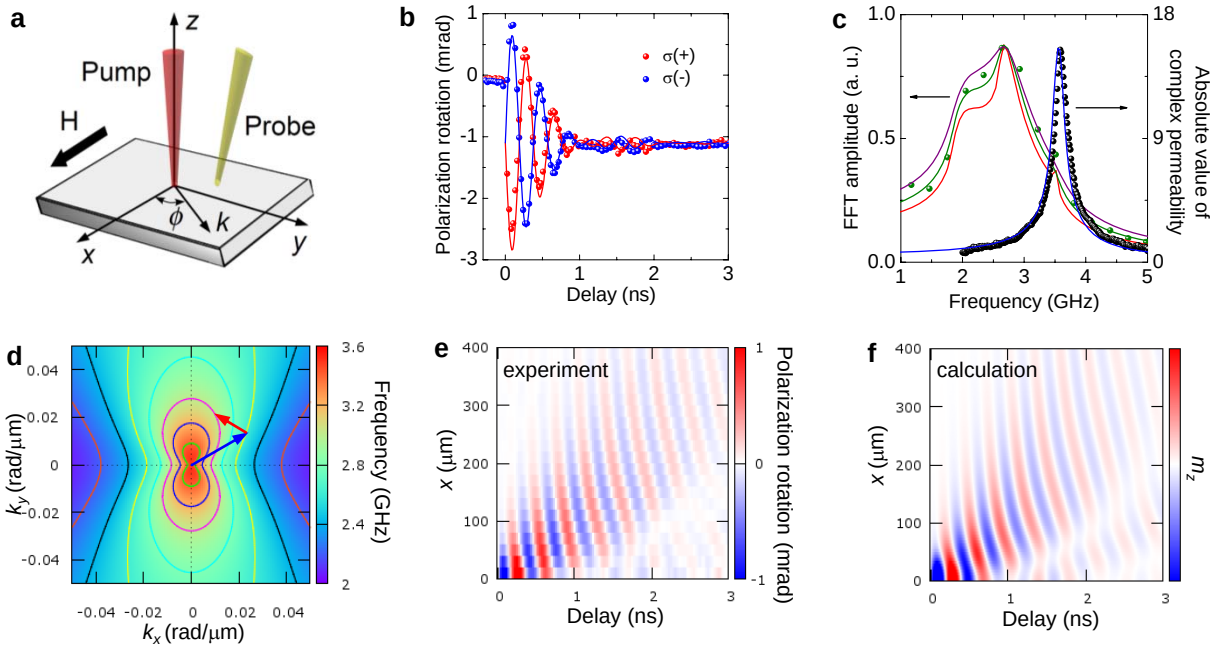

Figure 1 T. Satoh *et al.*, Nature Photonics

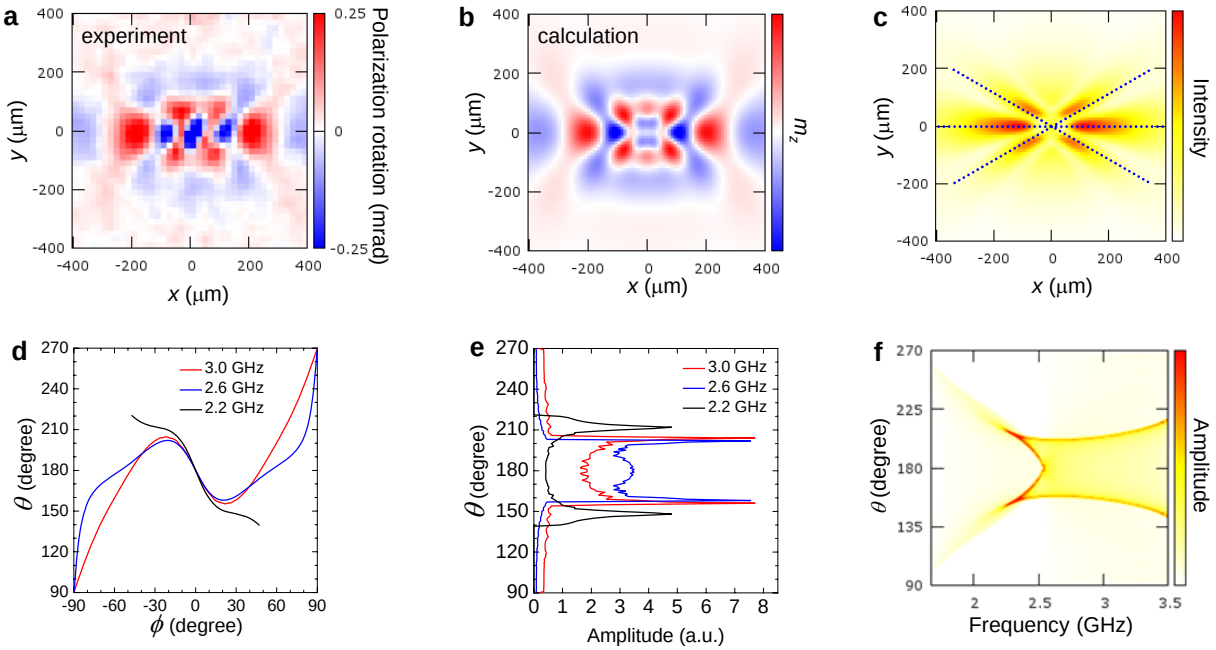

Figure 2 T. Satoh *et al.*, Nature Photonics

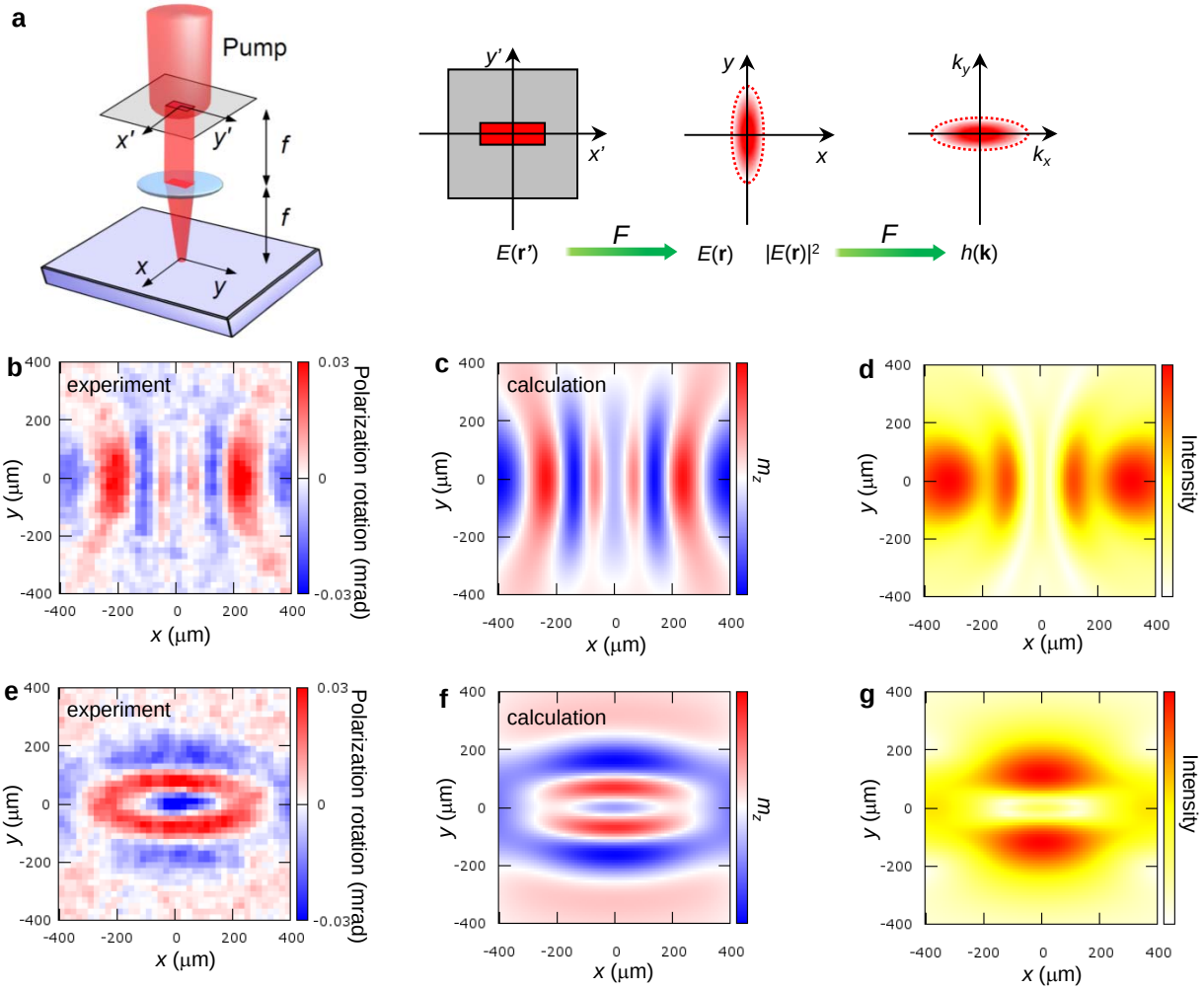

Figure 3 T. Satoh *et al.*, Nature Photonics